Compound eyes and retinal information processing in miniature dipteran species match their specific ecological demands

Paloma T. Gonzalez-Bellido[a,1], Trevor J. Wardill[a,1], and Mikko Juusola[a,b,2]

[a]Department of Biomedical Science, University of Sheffield, Sheffield S10 2TN, United Kingdom; and [b]State Key Laboratory of Cognitive Neuroscience and Learning, Beijing Normal University, Beijing 100875, China

The compound eye of insects imposes a tradeoff between resolution and sensitivity, which should exacerbate with diminishing eye size. Tiny lenses are thought to deliver poor acuity because of diffraction; nevertheless, miniature insects have visual systems that allow a myriad of lifestyles. Here, we investigate whether size constraints result in an archetypal eye design shared between miniature dipterans by comparing the visual performance of the fruit fly *Drosophila* and the killer fly *Coenosia*. These closely related species have neural superposition eyes and similar body lengths (3 to 4 mm), but *Coenosia* is a diurnal aerial predator, whereas slow-flying *Drosophila* is most active at dawn and dusk. Using in vivo intracellular recordings and EM, we report unique adaptations in the form and function of their photoreceptors that are reflective of their distinct lifestyles. We find that although these species have similar lenses and optical properties, *Coenosia* photoreceptors have three- to fourfold higher spatial resolution and rate of information transfer than *Drosophila*. The higher performance in *Coenosia* mostly results from dramatically diminished light sensors, or rhabdomeres, which reduce pixel size and optical cross-talk between photoreceptors and incorporate accelerated phototransduction reactions. Furthermore, we identify local specializations in the *Coenosia* eye, consistent with an acute zone and its predatory lifestyle. These results demonstrate how the flexible architecture of miniature compound eyes can evolve to match information processing with ecological demands.

vision | predatory behavior | invertebrate | evolution

The design of a compound eye depends on the limits imposed by body size, architectural properties of the eye, visual task, and habitat, all of which affect its ability to resolve environmental light patterns (1–3). Typically, compound eyes are roughly spherical in shape, sectored into arrays of lens-capped sampling units, named ommatidia, which accept light from narrow angles (3), determining their sampling resolution (4). Although the eye's sampling resolution can improve when its lenses shrink, their projected image blurs more because of diffraction (5). The optimal lens diameter, which is expected when these two limits nearly meet, scales with the square root of the eye size across many insect species (5), implying high resolution as their design objective. However, smaller lenses collect less light, reducing the signal-to-noise ratio (SNR) of the sampled image (4). Although the lenses perform light collection, the focal length of the lens and the diameter of the light guides, or rhabdomeres, finally determine the pixel size (6). In combination, lens diameter, rhabdomere width, and focal length impose a tradeoff between spatial resolution and sensitivity (intensity resolution), which is thought to be further aggravated the smaller the eyes (3, 7, 8).

Ultimately, because the demands for pattern recognition differ greatly for different visual tasks and habitats (9), the selected eye design should reflect the insect's lifestyle (3) and the versatility of neural information processing in its visual system (10). A fast-flying aerial predator needs to resolve rapidly changing information to detect food and partners, whereas a slow-flying crepuscular fructivore may have less urgent demands for its vision. Accordingly, compound eyes of many large insects show unique adaptations; their lens sizes and shapes can vary, including local specializations, such as bright or acute zones for increasing sensitivity or resolution (11), respectively, and their neural responses suggest tuning for the spatial and temporal characteristics of the light environment (12–14). However, given the severity of size constraints on optics, one is surprised to find a plethora of very small insects with a vast variety of visually challenging lifestyles. How can their miniature compound eyes allow such richness of visual behaviors? How has their visual information processing adapted to their different visual lifestyles?

We have begun finding answers to these open questions by investigating the optical and retinal adaptations of two miniature fly species with a similar body size and architectural properties (neural superposition eye). The predatory killer fly *Coenosia attenuata* (Muscidae, Coenossinae) and the fruit fly *Drosophila melanogaster* (Drosophilidae, Drosophilinae), which separated 120 million years ago (15), exhibit specialized behaviors requiring different spatiotemporal visual information. Killer flies can detect a flying prey in the presence of a complex background and perform a high-speed aerial capture, whereas fruit flies distinguish only relatively large and slowly moving objects (16, 17). Using in vivo intracellular recordings, scanning EM, and transmission EM (TEM), we show that although the lens diameter and optical properties are similar in both species, the spatial resolution and information transfer rate of *Coenosia* photoreceptors are three to four times higher than those of *Drosophila*. This performance is achieved by the smallest rhabdomeres ever reported in a flying insect, which (*i*) reduce blur and cross-talk between photoreceptors, improving spatial resolution as required for its predatory lifestyle, and (*ii*) incorporate microvillar phototransduction reactions with drastically reduced processing delays, enabling them to transmit even higher information rates than photoreceptors of much larger *Calliphora* flies. Furthermore, we report local specializations in the *Coenosia* eye consistent with an acute zone, evidencing that local specializations of the eye are not confined to larger animals.

Results

Visual Performance and Body Size. Our video footage confirmed previous field observations that *Coenosia* outperform *Drosophila* in visual flight control; *Coenosia* catch *Drosophila* midflight (Movie S1), consuming their prey after landing (Fig. 1 *A* and *B*). *Coenosia* have larger eyes than *Drosophila* (Fig. 1 *C–E*). In the case of male *Coenosia*, whose body size is similar to that of *Drosophila*, the larger eyes indicate a higher investment in the visual system. Larger eyes can support bigger and/or more sampling units and may provide the eye with a larger sampling area. However, if the sampling area stays constant and other eye parameters (i.e., focal length, rhabdomere width, etc.) are unchanged, larger and thus fewer lenses increase sensitivity by collecting light over a wider angle, at the expense of sampling resolution. The reverse also holds: boasting more but smaller lenses narrows the interommatidial angles, which improves the sampling resolution at the expense of sensitivity. To investigate how the larger eye of *Coenosia* is used, we counted and measured the lenses and gauged the interommatidial angles across the eyes of both species.

Lens Metrics and Interommatidial Angles. We found that *Coenosia* has two to three times more lenses than *Drosophila*, but their average sizes are similar (Table S1). Although the *Drosophila* eye shows no obvious regional specializations (lens diameter = 16.85 μm ± 0.21 SEM), the lens diameter of *Coenosia* increases significantly from the posterior toward the front of the eye, yielding values between 14 and 20 μm ($P < 10^{-5}$) for females and between 13 and 17 μm ($P < 10^{-5}$) for males (Fig. 2*A*). The larger frontal lenses of *Coenosia* indicate local specializations for either increased sensitivity (bright zone) or resolution (acute zone).

To determine whether *Coenosia*'s frontal lenses sample the environment at higher spatial frequencies than (*i*) the remainder

Fig. 2. Lens diameter (D) and interommatidial angle (Δφ) across the eyes (miniature figures to the right indicate the sectioning plane used for each graph). (*A*) Eyes were divided into anterior, lateral, and posterior regions and the respective lens diameters measured from several locations for each region (n = 1 for each genotype). For each location, the mean distance (n = 5) between the center of neighboring lenses is plotted on the x axis, according to their estimated horizontal position. (*B*) Mean interommatidial angles from horizontal cuts of ♀ *Coenosia* and *Drosophila*. *Coenosia* have the smallest Δφ in the anterior (frontal) region (Δφ = 1.88°) (n = 2). (*C*) Even when the center of the acute zone is not sectioned (Fig. S2*A*), mean Δφ in *Coenosia* reach smaller values than *Drosophila* (n = 2 for each genotype). (Scale bars, 200 μm.)

Fig. 1. Comparing *Coenosia attenuata* and *Drosophila melanogaster* sizes. (*A* and *B*) *Coenosia* ♀ and ♂, respectively, with *Drosophila* prey, previously caught midflight (Movie S1). (*C–E*) Anterior-dorsal scanning EM views from heads of *Drosophila* and *Coenosia* ♀ and ♂, respectively. The eye of *Coenosia* is larger than that of *Drosophila* and contains more ommatidia. (Scales bars, 250 μm.)

of the *Coenosia* eye and (*ii*) *Drosophila* frontal lenses, we measured the interommatidial angles (Δφ), which describes the cornea sampling density (18). Using semithin horizontal sections from resin-embedded samples, we located the smallest interommatidial angles at the front of the *Coenosia* eye (Δφ = 2.2° ± 0.08 SEM; Fig. 2*B*), where the cornea curvature is flatter (Fig. S1*A*). Thus, in *Coenosia*, the lowest Δφ values match the area of increased lens diameter, where the pseudocone and rhabdomere are longest (Fig. S1*A*), implying the presence of a frontal acute zone. In contrast in *Drosophila*, the smallest interommatidial angles were found in the lateral part of the eye (Δφ = 4.5° ± 0.08 SEM; Fig. 2*B* and Fig. S1*B*). Nonetheless, we further measured Δφ from oblique cuts (Fig. 2*C*), following one row of ommatidia (Fig. S2 *A* and *B*) to prevent any bias in the species comparison, because *Muscoid* (including *Coenosia*) lenses change orientation and shape horizontally (19) (Fig. S2 *C* and *D*). In the posterior area of the eye, Δφ is similar between *Coenosia* and *Drosophila* (Fig. 2*C*), but its gradient is largest in *Coenosia*, where Δφ reaches 2.20°. In contrast, the smallest Δφ in *Drosophila* is 3.38°, and for two thirds of its eye Δφ > 4°. Therefore, in *Coenosia*, the lens array achieves a higher spatial sampling frequency than in *Drosophila*. In the lateral region of the eye, where the sampling density is highest along this cut, the Δφ values for male and female *Coenosia* are similar (P = 0.425). Thus, although *Coenosia* males have smaller eyes than females, the male's spatial sampling frequency is not reduced because the whole eye ensemble maintains similar proportions (8).

Spatial Resolving Power of Photoreceptors. The optics suggests that the *Coenosia* eye evolved for increased spatial resolution, with its

denser sampling providing potential for a smaller "pixel" size. However, acuity improvements can only be realized if matched neurally in the retina, which requires narrowing the field of view of each photoreceptor. To test whether the acuity of R1–R6 photoreceptors in *Coenosia* is higher than in *Drosophila*, we measured intracellularly their responsiveness to light stimuli delivered from different spatial angles (Fig. 3*A*). We then gauged the half-width of these angular sensitivity functions, or the acceptance angle ($\Delta\rho$), to describe their spatial resolution. We discovered that photoreceptors in *Coenosia,* collect light from significantly smaller fields ($^{\female}\Delta\rho = 2.88° \pm 0.07$; $^{\male}\Delta\rho = 2.59° \pm 0.10$ SEM) than in *Drosophila* ($\Delta\rho = 8.23° \pm 0.54$) ($P < 10^{-5}$; Table S1). Because male and female *Coenosia* showed similar spatial resolution ($P = 0.124$), their different eye sizes had little impact on their retinal acuity.

Retinal Morphology Matches Lifestyle. How has the eye morphology of *Drosophila* and *Coenosia* evolved to support their ex-

tremely different spatial visual performances? The angular sensitivity of a photoreceptor is determined by the diameter of the lens and by the angular size of the rhabdomere (20–22). Because the lens diameters, and therefore their Airy disk projections, are similar in both species (Table S2), the large difference in visual performance between *Coenosia* and *Drosophila* cannot be explained by diffraction limitations. In diffraction-limited eyes, the acceptance angle of a single photoreceptor should equal the half-width of the Airy disk (20), but this condition is not met by either species. Therefore, the angular size of the rhabdomere, a product of the focal length and the distal rhabdomere tip diameter, must provide the means to match the spatial resolution recorded intracellularly.

We measured, by the cornea-drop method (23), the focal length of the lenses in the lateral region of female eyes (Table S1). Although the focal length is longer in *Coenosia* than in *Drosophila*, their differences were too small to account for the recorded difference in spatial performance. In contrast, we dis-
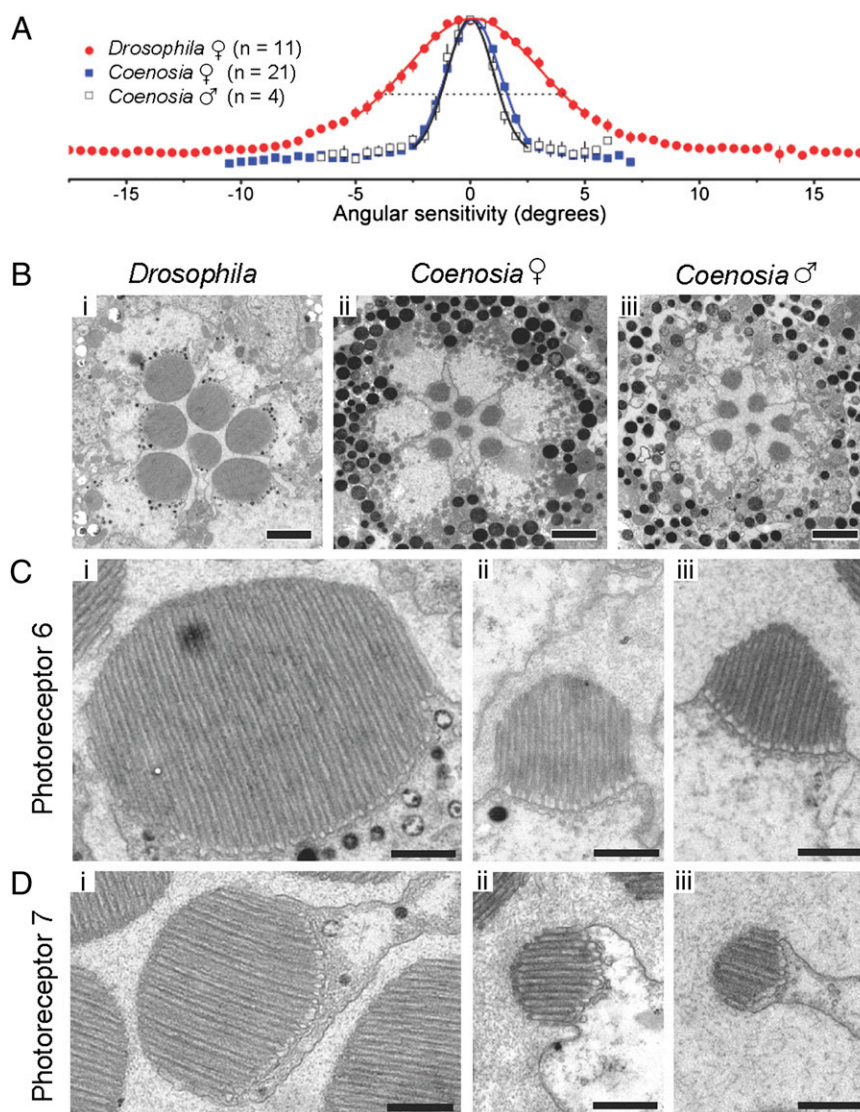
Fig. 3. Spatial resolution and TEM micrographs of photoreceptors. (*A*) Spatial resolution of nearly dark-adapted acceptance angle ($\Delta\rho$) for *Drosophila* and *Coenosia*. Mean angular sensitivity functions of female *Drosophila* and *Coenosia* ♀ and ♂ data fitted with Gaussians. For *Drosophila* $\Delta\rho = 8.23°$, *Coenosia* ♀ $\Delta\rho = 2.88°$, and ♂ $\Delta\rho = 2.59°$. (*B*) Cross-sections of the distal ommatidia, just below the photoreceptors caps, in the lateral eye regions. (Scale bars, 2 μm.) (*C*) R6 rhabdomeres are shown as examples for R1–R6 photoreceptors. Male *Coenosia* rhabdomeres exhibit a "pyramidal" shape. (Scale bars, 500 nm.) See Table S1 for rhabdomere dimensions. (*D*) R7 Rhabdomeres are shown. (Scale bars, 500 nm.) See Table S1 for rhabdomere dimensions.

covered from TEM cross-section images that the distal major and minor diameters of R1–R6 rhabdomeres in *Drosophila* are twice as large as those of *Coenosia* (Fig. 3 *B* and *C*; d_{major}: 2.34 vs. 1.10 (♀) or 0.96 (♂) μm, respectively, $P_{majord} < 10^{-5}$). This ratio is also clear in R7 (Fig. 3*D*; d_{major}: 1.75 vs. 0.83 (♀) or 0.70 (♂) μm, respectively, $P_{majord} < 10^{-5}$). Furthermore, the rhabdomeres in *Coenosia* males are significantly smaller than in females ($P_{R1–R6} < 10^{-5}$; $P_{R7} = 0.000152$). These sections were cut perpendicular to the rhabdomere axis, as shown by the parallel arrangement of the microvilli (Fig. 3 *C* and *D*), so these findings are not artifacts due to oblique sectioning. Because the width of each microvillus appears fairly constant across the genotypes, the size and shape differences between their rhabdomeres are determined by the length and number of the microvilli.

To enhance the resolving power of photoreceptors, some predatory insects have smaller rhabdomeres in their acute zones (6, 24). To quantify whether such adaptation is also apparent in *Coenosia*, we used TEM to image cross-sections of the ommatidia in the frontal eye region. Here, the male R1–R6 rhabdomeres were also smaller than those of the females ($P_{R1–R6} = 3 \times 10^{-5}$; Table S3), but the major diameter of the rhabdomeres did not change significantly between the lateral and the frontal areas ($^{♀}P_{R1–R6} = 0.389$; $^{♂}P_{R1–R6} = 0.990$). It is feasible that the rhabdomere dimensions in the lateral region of the retina already approximate the functional limit for a light-propagating structure. Horridge et al. (20) estimated that for fly rhabdomeres this limit is 0.7 μm, which is the R7/R8 major rhabdomere width of killer flies. Very narrow wave-guides propagate a large proportion of their light outside their boundaries, but short wavelengths of light are still carried within the waveguide (25). Hence, for efficient photon capture, there is likely a selection pressure to use short-wavelength absorption pigments in thin rhabdomeres. Additionally, the major diameter of the R7 rhabdomeres was significantly larger in the frontal zone ($^{♀}P_{R7} = 0.00665$; $^{♂}P_{R7} = 0.00148$; Table S2). A similar assembly is seen in the fronto-dorsal "love spot" of the male housefly, where the unique blue-green–sensitive R7 photoreceptors terminate in the lamina, instead of traveling to the medulla (26). This wiring variation is thought to increase sensitivity (26).

In addition to their absolute size, the spacing between the boundaries of neighboring rhabdomeres can influence the final spatial resolution of the fly retina, because the cross-talk between waveguides depends on their relative rhabdomere distance (20, 27). It has been extrapolated that only when the value of such relative distance (*cross-talk index*; SI Materials and Methods) is >3, the light transfer between rhabdomeres remains below a few percent, and the excitation in neighboring waveguides can be considered independent (27). To establish cross-talk index in the two species and sexes, we measured in the lateral part of the eye the major and minor diameter of the rhabdomeres, and the distances between neighboring photoreceptors, at two depth levels within an ommatidium (Table S4). Cross-talk index at the distal level was <3 for all three specimens, similar to *Musca* (27). At the waist of the ommatidium (near the interface between R7 and R8), *Coenosia* changes the relative distance of its rhabdomeres to >3.5, but the *Drosophila* index is still <2.3 at the same depth, which should permit significant cross-talk between rhabdomeres. Moreover, longitudinal sections in the *Coenosia* eye reveal a higher density of screening pigment than in the *Drosophila* eye (Fig. S1 *C* and *D*). Thus, the deterioration in spatial resolution by stray light is likely to impact *Drosophila* more than *Coenosia*.

The final spatial detail acquired by the eye depends on the amount of overlap between the angular sensitivity of adjacent photoreceptor cells, which is described by the Δρ/Δφ ratio (6). In *Calliphora*, the interommatidial angle and the acceptance angles are matched (13), which results in Δρ/Δφ ≈ 1; this value is common among fast-flying diurnal dipterans (3). In nearly dark-adapted *Coenosia* females Δρ(mean)/Δφ(median) ≈ 2.8/2.8 = 1, which matches well with its predatory, diurnal, and fast-flying characteristics. In contrast, many crepuscular and nocturnal animals display Δρ >> Δφ, meaning an extended overlap between photoreceptor visual fields (3). Such a ratio increases the reliability of the signal (SNR) and produces a brighter image (23, 26, 28); both are helpful in low lighting conditions (23). Thus, the ratio for nearly dark-adapted *Drosophila*, Δρ(mean)/Δφ(median) = 8.23/4.63 = 1.77, is consistent with a crepuscular ecology.

Temporal Resolving Power of Photoreceptors. The photoreceptors of large diurnal dipteran flies have faster temporal properties than those of *Drosophila* (14, 17, 29). *Drosophila* is most active at twilight, when photoreceptors integrate light over prolonged periods to form reliable images. In contrast, large diurnal dipterans can afford faster image integration because they prefer brighter environments and because their larger ommatidia can collect more photons. *Coenosia* is a fast-flying diurnal muscoid, with predatory habits, that needs fast photoreceptors to prevent blurred vision during acrobatic hunts. However, its small head can only host relatively short photoreceptors, which coupled to a small lens and a narrow angular sensitivity could result in the sampled images having a low SNR.

We first quantified the temporal resolving power of R1–R6 photoreceptors in these miniature eyes, by examining their voltage responses to light stimuli in briefly dark- and light-adapted conditions (Fig. 4 *A* and *B*, respectively). We found that *Coenosia* photoreceptors generate exceptionally brief voltage responses, which rise and decay approximately three times faster than those of *Drosophila* (Fig. 4*A* and *B*). Here, latency, an electrically silent period in which intracellular phototransduction reactions amplify and convey the message of photon-capture to ion-channel openings on the plasma membrane (17), is >50% briefer in similarly dark-adapted *Coenosia* photoreceptors (*Coenosia*: 2.8 ms ± 0.5; *Drosophila*: 6.2 ms ± 0.8 SD; Fig. S3 *A* and *B*). *Coenosia* thus has significantly faster phototransduction reactions than those in *Drosophila* ($P < 10^{-7}$). We next tested how their response dynamics compare with those of larger muscoid flies, which have very fast eyes (14), by repeating the experiments in R1–R6 blowfly (*Calliphora vicina*) photoreceptors. We discovered that the *Coenosia* phototransduction operates significantly faster than that of *Calliphora* ($P < 2.7 \times 10^{-5}$), when briefly dark- and light-adapted (Fig. 4 *A* and *B*, respectively).

However, fast responses can be noisy, owing to limitations of unreliable hardware or low sampling, and so carry little neural information. We therefore measured how well their phototransduction reactions can represent natural light patterns (i.e., code different stimulus patterns as different by their voltage responses) (Fig. 4*C* and Fig. S3 *D–I*). We found that *Drosophila* photoreceptors encode reliably slow stimulus changes (≤43 Hz ± 2 SD, SNR(*f*) > 1), whereas *Coenosia* photoreceptors could do so with stimuli more than fourfold faster (≤186 ± 12 Hz). *Coenosia*'s responses further exceed those of *Calliphora*, which could encode the same stimulus reliably until 132 ± 11 Hz. Finally, we calculated the rate of information transfer (29) of these responses (Fig. 4*D*). Here, *Drosophila* photoreceptors transmitted on average 260 bits per second, and those of *Coenosia* and *Calliphora* were 885 and 639 bits per second, respectively. *Drosophila* and *Calliphora* data concur with previous reports (29, 30).

We now recall two ways to increase a photoreceptor's rate of information transfer, when noise is not limiting (31) (Fig. 4 *C* and *D*). One can either capture more photons by adding more sampling units (microvilli) (17, 32) or reduce processing delays in microvillar phototransduction reactions (7, 33). In the former case, the rhabdomere grows, whereas in the latter it may shrink. The short microvilli of *Coenosia* photoreceptors (Fig. 3 *C* and *D*) should reduce diffusion distances and accelerate phototransduction by reducing latency, similar to warming (33). This
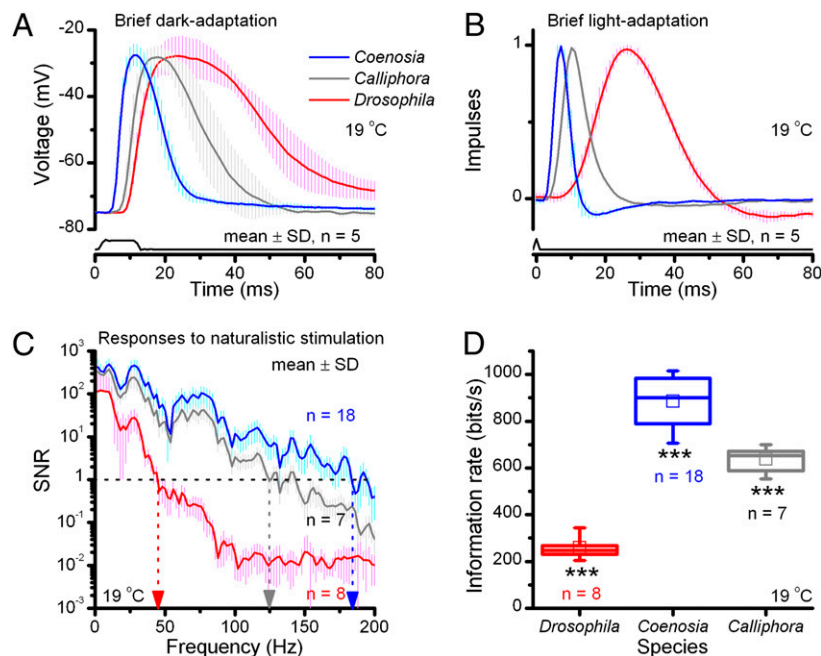
NEUROSCIENCE

Fig. 4. Temporal resolution of R1–R6 photoreceptors. (*A*) Responses of five briefly dark-adapted *Coenosia*, *Calliphora*, and *Drosophila* photoreceptors to a 10-ms saturating light pulse. (*B*) Normalized impulse responses of five briefly light-adapted photoreceptors to a pseudorandom contrast. (*C*) SNR of voltage responses to a repeated presentation of bright natural light intensity series. High SNRs (>100) at low frequencies, in which most of the power of natural images resides, implies that signaling is not limited by phototransduction noise. (*D*) Information transfer of the same responses as in C, calculated as the difference between their entropy and noise entropy (Fig. S3).

result is independent of the filtering properties of the plasma membrane, because response integration in short *Coenosia* microvilli is much faster than in long *Calliphora* microvilli, although their membrane time constants and impedances are similar (Fig. S3B; *SI Materials and Methods*). Naturally, other molecular adaptations, which do not need to be mutually exclusive, may also reduce their processing delays.

Discussion

Our results provide insights regarding how the architectural properties of very small eyes and the form and function of their photoreceptors affect neural coding and vision at the physical limit imposed by light-propagating structures. Specifically, our findings indicate that the retinal adaptations of miniature dipterans are consistent with what we know about their ecology and lifestyle. *Coenosia* favors resolution over sensitivity, perhaps so that prey items can be recognized and targeted with precision. In contrast, the eye of *Drosophila* has adapted to improve light capture, which helps to reconstruct an image under low lighting conditions even though the details may not be well resolved. Although their body sizes are similar, *Coenosia* achieves higher resolution because of more sampling units, smaller interommatidial angles, narrower rhabdomeres, and lower cross-talk than those found in *Drosophila*. *Coenosia*'s R1–R6 rhabdomere diameter is possibly the smallest ever reported for an insect, smaller than in hoverflies (20), and correspondingly its phototransduction reactions are considerably faster than those of *Drosophila*, enabling them to transmit even more information than much larger *Calliphora* photoreceptors.

Importantly for the field of sensory evolution, our data clarify that the poor spatial resolving power of *Drosophila* photoreceptors ($\Delta\rho = 8.23°$) is not a selective outcome of evolving a small body or head, or diffraction-limited optics. Instead, it is more likely to reflect the low light availability during *Drosophila*'s preferred activity period, with its uniform lenses (15–18 µm) highlighting the generalist nature of its vision. Had *Drosophila* maximized the

available space for resolution, its lenses would be at least as small as those of male *Coenosia* (13 µm), and their acceptance angle would approach the Airy disk half-width. Appropriately for sensitivity selection, in *Drosophila*, the distal diameter of rhabdomeres, which shapes the range of angles a photoreceptor accepts incident light (20, 21), is similar or larger than in *Musca* and *Calliphora*, appearing immense compared with that of *Coenosia*. The reduced pigmentation within *Drosophila* ommatidia, which subsequently may cause off-axis illumination and cross-talk, can be viewed as a positive adaptation for crepuscular lifestyle. Matching these architectural properties, *Drosophila* photoreceptors operate slowly and follow low frequencies best when stimulated with a bright naturalistic time series (*SI Materials and Methods*), whereas their voltage-sensitive membranes filter the remaining high-frequency noise (17).

Furthermore, our *Coenosia* data demonstrate that local specializations of the eye are not limited by diffraction, nor are they confined to larger animals. Its predatory nature is well reflected by the frontal area of its eye, which shows increased lens diameters, reaching 20 µm in the female. Nonetheless, these lenses are small compared with those of fast-flying blowflies (20–80 µm) (34) and hoverfly (26–40 µm) (35). Hence, the small lens diameter of *Coenosia* can be viewed as a compromise to achieve high acuity with a small eye. Together, smaller rhabdomeres and larger lenses should aid detection of small targets by causing large input fluctuations in the photoreceptor array when the target moves (11), yet by selecting small lenses its eye packs in more sampling units. In the frontal region of the eye, where higher acuity is a premium, we did not find smaller R1–R6 rhabdomeres. There instead, R7 rhabdomeres are wider than anywhere else in the eye, for both female and male specimens, similar to the acute zone of male *Musca* (26). Thus, our results suggest that the rhabdomere dimensions, and thus their waveguide properties, might have been selected for improved quantum capture at the spectral excitation range of the imbedded photopigments.

From a neural computation point of view, the strikingly fast speed and very high SNR (>500 in some frequencies) of *Coenosia* photoreceptor output clarify that selecting small eyes for predatory lifestyle does not mean compromising their temporal resolution. Nonetheless, such impressive visual performance seems to be energetically expensive (36). In retinal TEM sections, the number of mitochondria in each *Coenosia* photoreceptor appears to systematically outnumber those in *Drosophila* (Fig. S4 *A* and *B*), suggesting that fast *Coenosia* photoreceptors are more metabolically active and therefore more costly to maintain than the slow *Drosophila* photoreceptors.

Materials and Methods

Fruit flies (*Drosophila melanogaster*) were raised at 18 °C in a 12-h/12-h dark/light cycle. Wild-type stocks were from Bloomington Stock center, and only females were used. Adult *Coenosia attenuata* were collected in greenhouses in Almeria (Spain) April–May 2009 and July 2010. In captivity, *Coenosia* were kept at ≈24 °C and fed live *Drosophila* and *Lycoriella auripila*.

The dissection and fixation protocols for EM were as previously described (28). For light microscopy, tissues were prepared as described for the TEM sections. Semithin sections of 0.2- to 0.5-μm thickness were obtained and stained with 1% Toluidine Blue dissolved in 1% Borax. The samples were viewed and photographed with a ScanScope GL scanner (Aperio Technologies). How lens and photoreceptor diameters were measured is described in Fig. S4 *C* and *D*. Semithin (0.5-μm) longitudinal sections were cut horizontally (antennae to neck; Fig. 2*B*) and diagonally along an ommatidia row, which crossed the eye from posterior to anterior in the medial part of the eye (Fig. 2*C*). The interommatidial angles from five neighboring ommatidia were averaged (±SEM). Focal length was measured experimentally as previously described (23) (Fig. S4*E*).

We recorded intracellularly from R1–R6 photoreceptors in the *Drosophila* and *Coenosia* retina at 19 °C with sharp quartz microelectrodes (120–220 MΩ with 3 M KCl) pulled on a Sutter P2000 electrode puller. Once dark-adapted, their voltage responses to light pulses of varying intensity were characterized according to their receptive fields; whereas their responses to bright white-noise modulated luminance contrast or naturalistic light intensity series (9) were examined as previously described (17, 29). Data were sampled at 1 to 2 kHz with a National Instruments 12-bit A/D converter and analyzed offline with a custom-built MATLAB interface. Details in *SI Materials and Methods*.

1. Land MF, Fernald RD (1992) The evolution of eyes. *Annu Rev Neurosci* 15:1–29.
2. Warrant EJ, McIntyre PD (1993) Arthropod eye design and the physical limits to spatial resolving power. *Prog Neurobiol* 40:413–461.
3. Land MF (1997) Visual acuity in insects. *Annu Rev Entomol* 42:147–177.
4. Snyder AW, Stavenga DG, Laughlin SB (1977) Spatial information capacity of compound eyes. *J Comp Physiol A Neuroethol Sens Neural Behav Physiol* 116:183–207.
5. Barlow HB (1952) The size of ommatidia in apposition eyes. *J Exp Biol* 29:667–674.
6. Horridge GA, Duelli P (1979) Anatomy of the regional differences in the eye of the mantis *Ciulfina*. *J Exp Biol* 80:165–190.
7. Howard J, Snyder AW (1983) Transduction as a limitation on compound eye function and design. *Proc R Soc Lond B Biol Sci* 217:287–307.
8. Kirschfeld K (1976) The resolution of lens and compound eyes. *Neural Principles of Vision*, eds Zettler F, Weiler R (Springer, New York), pp 356–370.
9. van Hateren JH (1997) Processing of natural time series of intensities by the visual system of the blowfly. *Vision Res* 37:3407–3416.
10. van Hateren JH (1992) A theory of maximizing sensory information. *Biol Cybern* 68:23–29.
11. Land MF (1998) Compound eye structure: Matching eye to environment. *Adaptive Mechanisms in the Ecology of Vision*, eds Archer S, Djamgoz MB, Loew E, Partridge JC (Kluwer Academic Publishers, London), pp 51–72.
12. Burton BG, Tatler BW, Laughlin SB (2001) Variations in photoreceptor response dynamics across the fly retina. *J Neurophysiol* 86:950–960.
13. Hardie RC (1985) Functional organization of the fly retina. *Progress in Sensory Physiology*, ed Ottoson D (Springer, New York), Vol 5, pp 1–79.
14. Laughlin SB, Weckström M (1993) Fast and slow photoreceptors—a comparative study of the functional diversity of coding and conductances in the Diptera. *J Comp Physiol A Neuroethol Sens Neural Behav Physiol* 172:593–609.
15. Dübendorfer A, Hediger M, Burghardt G, Bopp D (2002) *Musca domestica*, a window on the evolution of sex-determining mechanisms in insects. *Int J Dev Biol* 46:75–79.
16. Buchner E, Götz KG, Straub C (1978) Elementary detectors for vertical movement in the visual system of *Drosophila*. *Biol Cybern* 31:235–242.
17. Juusola M, Hardie RC (2001) Light adaptation in *Drosophila* photoreceptors: I. Response dynamics and signaling efficiency at 25 °C. *J Gen Physiol* 117:3–25.
18. Stavenga DG (2006) Invertebrate photoreceptor optics. *Invertebrate Vision*, eds Warrant EJ, Nilsson DE (Cambridge Univ Press, Cambridge, UK).
19. Stavenga DG (1975) The neural superposition eye and its optical demands. *J Comp Physiol* 102:297–304.
20. Horridge GA, Mimura K, Hardie RC (1976) Fly photoreceptors III. Angular sensitivity as a function of wavelength and limits of resolution. *Proc R Soc Lond B Biol Sci* 194: 151–177.
21. Stavenga DG (2003) Angular and spectral sensitivity of fly photoreceptors. II. Dependence on facet lens F-number and rhabdomere type in *Drosophila*. *J Comp Physiol A Neuroethol Sens Neural Behav Physiol* 189:189–202.
22. Wehner R (1975) Pattern recognition. *The Compound Eye and Vision of Insects*, ed Horridge GA (Clarendon Press, Oxford), pp 75–112.
23. Warrant EJ, et al. (2004) Nocturnal vision and landmark orientation in a tropical halictid bee. *Curr Biol* 14:1309–1318.
24. Rossel S (1979) Regional differences in photoreceptor performance in the eye of the praying mantis. *J Comp Physiol A Neuroethol Sens Neural Behav Physiol* 131:95–112.
25. Snyder AW, Miller WH (1972) Fly colour vision. *Vision Res* 12:1339–1396.
26. Hardie RC, Franceschini N, Ribi W, Kirschfeld K (1981) Distribution and properties of sex-specific photoreceptors in the fly *Musca domestica*. *J Comp Physiol A Neuroethol Sens Neural Behav Physiol* 145:139–152.
27. Wijngaard W, Stavenga DG (1975) On optical crosstalk between fly rhabdomeres. *Biol Cybern* 18:61–67.
28. Meinertzhagen IA, O'Neil SD (1991) Synaptic organization of columnar elements in the lamina of the wild type in *Drosophila melanogaster*. *J Comp Neurol* 305:232–263.
29. Juusola M, de Polavieja GG (2003) The rate of information transfer of naturalistic stimulation by graded potentials. *J Gen Physiol* 122:191–206.
30. Zheng L, et al. (2006) Feedback network controls photoreceptor output at the layer of first visual synapses in *Drosophila*. *J Gen Physiol* 127:495–510.
31. Shannon CE (1948) A mathematical theory of communication. *Bell Syst Tech J* 27: 379–423, 623–656.
32. Howard J, Blakeslee B, Laughlin SB (1987) The intracellular pupil mechanism and photoreceptor signal: Noise ratios in the fly *Lucilia cuprina*. *Proc R Soc Lond B Biol Sci* 231:415–435.
33. Juusola M, Hardie RC (2001) Light adaptation in *Drosophila* photoreceptors: II. Rising temperature increases the bandwidth of reliable signaling. *J Gen Physiol* 117:27–42.
34. Stavenga DG, Kruizinga R, Leertouwer HL (1990) Dioptrics of the facet lenses of male blowflies *Calliphora* and *Chrysomyia*. *J Comp Physiol A Neuroethol Sens Neural Behav Physiol* 166:365–371.
35. Straw AD, Warrant EJ, O'Carroll DC (2006) A "bright zone" in male hoverfly (*Eristalis tenax*) eyes and associated faster motion detection and increased contrast sensitivity. *J Exp Biol* 209:4339–4354.
36. Laughlin SB, de Ruyter van Steveninck RR, Anderson JC (1998) The metabolic cost of neural information. *Nat Neurosci* 1:36–41.

NEUROSCIENCE